Altered localization of *Drosophila* Smoothened protein activates Hedgehog signal transduction

Alan Jian Zhu, Limin Zheng, Kaye Suyama, and Matthew P. Scott[1]

Departments of Developmental Biology and Genetics, Howard Hughes Medical Institute, Beckman Center B300, Stanford University School of Medicine, Stanford, California 94305-5329, USA

Hedgehog (Hh) signaling is critical for many developmental events and must be restrained to prevent cancer. A transmembrane protein, Smoothened (Smo), is necessary to transcriptionally activate Hh target genes. Smo activity is blocked by the Hh transmembrane receptor Patched (Ptc). The reception of a Hh signal overcomes Ptc inhibition of Smo, activating transcription of target genes. Using *Drosophila* salivary gland cells in vivo and in vitro as a new assay for Hh signal transduction, we investigated the regulation of Hh-triggered Smo stabilization and relocalization. Hh causes Smo to move from internal membranes to the cell surface. Relocalization is protein synthesis-independent and occurs within 30 min of Hh treatment. Ptc and the kinesin-related protein Costal2 (Cos2) cause internalization of Smo, a process that is dependent on both actin and microtubules. Disruption of endocytosis by dominant negative dynamin or Rab5 prevents Smo internalization. Fly versions of Smo mutants associated with human tumors are constitutively present at the cell surface. Forced localization of Smo at the plasma membrane activates Hh target gene transcription. Conversely, trapping of activated Smo mutants in the ER prevents Hh target gene activation. Control of Smo localization appears to be a crucial step in Hh signaling in *Drosophila*.

[*Keywords*: Hedgehog; Patched; Smoothened; *Drosophila*]

Supplemental material is available at http://www.genesdev.org.

Received February 5, 2003; revised version accepted March 26, 2003.

Hedgehog (Hh) signaling controls many events in animal development, notably embryonic segmentation and imaginal disc patterning in flies, and limb growth and pattern, neural tube cell fate determination, cerebellar growth, skin development, and many other processes in vertebrates (for review, see Bailey et al. 2000; Ingham and McMahon 2001). The Hh receptor, Patched (Ptc), is antagonistic to its Hh ligand. In fly imaginal discs, Ptc restrains growth whereas a local source of Hh signal overcomes the restraining influence of Ptc and transiently stimulates growth. At the same time, Hh induces transcription of the *ptc* gene, thereby setting in motion a feedback control system in which the build-up of Ptc limits the effects of the Hh signal. This relationship is preserved in mammals, with induction of *ptc1* being a signature effect of all three Hh family members in most tissues. The restraining influence of Ptc1 is most clearly visible in the skin and the cerebellum. Loss of one copy of *ptc1* in mice and humans increases the frequency of basal cell carcinoma of the skin and medulloblastoma, a tumor of the cerebellum. The normal role of Shh in the cerebellum is as a powerful but transient mitogen, but if Ptc1 function is reduced, growth can become uncontrolled.

The roles of Hh signaling in many processes of medical and developmental significance make understanding Hh signal transduction imperative. Although some variations have been noted, the following incorporates most findings to date (for review, see Nybakken and Perrimon 2002). Ptc appears to be a 12-transmembrane protein; Smoothened (Smo), a seven-transmembrane protein related to the Frizzled class of Wnt receptors. When Hh binds to Ptc, Smo is somehow unleashed to begin the process of activating target gene transcription. The way in which Ptc inhibits and Hh activates Smo protein appears to be posttranscriptional, but the mechanism is unknown. Despite the seemingly familiar structure of Smo, little evidence has been obtained for typical G protein transduction and the events immediately downstream of Smo remain a mystery.

smo is transcribed in a broad pattern and does not appear to be transcriptionally regulated by the Hh signal. Smo protein is posttranscriptionally regulated by becoming phosphorylated and more stable, and by moving to the cell surface after a Hh signal is received (Alcedo et al.

[1]**Corresponding author.**
E-MAIL scott@cmgm.stanford.edu; FAX (650) 725-7739.
Article published online ahead of print. Article and publication date are at http://www.genesdev.org/cgi/doi/10.1101/gad.1080803.

2000; Ingham et al. 2000; Denef et al. 2000). Although flies provide powerful genetic tools for studying the Hh signaling cascade, cells of fly embryos and imaginal discs are small enough to impede analysis of protein subcellular localization. Here we show that *Drosophila* salivary gland cells, a much larger cell type, are responsive to Hh signaling. We have used these cells for in vivo studies and in vitro pharmacological treatments to analyze the regulation and meaning of the dramatic intracellular movements of Smo that occur in response to Hh.

Results

Functional tests of Smo and GFP–Smo during embryonic and wing development

To meaningfully analyze changes in the intracellular location of Smo protein, we used in vivo tests to establish that a green fluorescent protein (GFP)-tagged Smo protein is active. *smo* and *gfp–smo* (*gsmo*) transgenes were expressed using a GAL4-responsive UAS promoter in transgenic flies. Strong evidence for the ability of GFP–Smo to function like wild-type Smo came from rescue of mutant embryos. Both wild-type *smo* and *gfp–smo*, driven by *da*–GAL4, were able to rescue the cuticle phenotype in a *smo*-null (smo^3) background (Quirk et al. 1997; Fig. 1, cf. C,D and A), whereas GFP alone had no rescuing ability (Fig. 1B). Therefore, GFP-tagged Smo is active and can function much like untagged protein.

As a second measure of GFP–Smo function, a GAL4 transgene (71B) that is expressed broadly though not uniformly in the wing imaginal disc (Fig. 1I) was used to produce Smo at higher than normal levels, in addition to the endogenous Smo. Expression of both tagged and untagged Smo results in an extra cross-vein between L2 and L3 in 10%–20% of the progeny (Supplementary Fig.

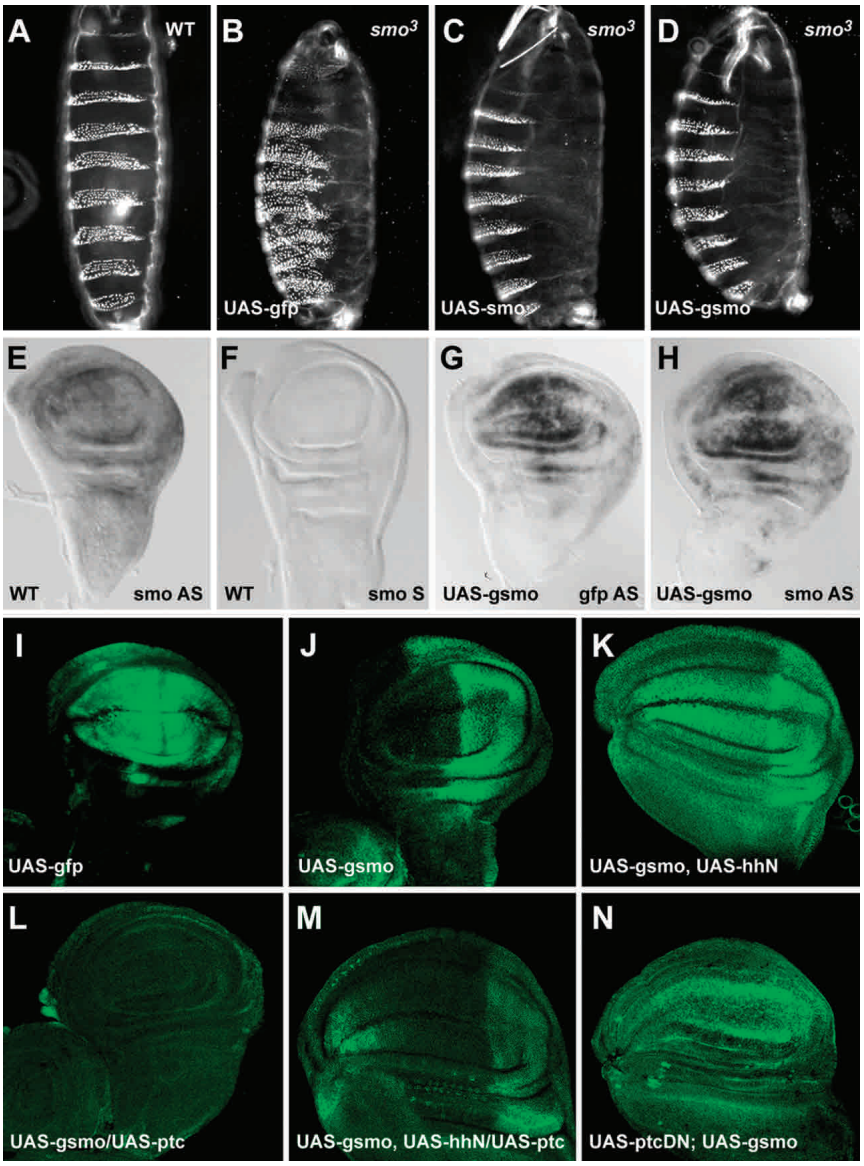

Figure 1. Posttranscriptional regulation of Smo by Hh and Ptc. (*A–D*) Cuticle preparation of a wild-type embryo (*A*) and smo^3 homozygotes expressing *gfp* (*B*), *smo* (*C*), or *gfp–smo* (*D*), using *da*–GAL4. (*B*) The typical zygotic null phenotype at 18°C; a continuous lawn of denticles covering most of the ventral surface. (*E–H*) In situ hybridization of wing discs from wild-type (*E,F*) and the 71B–-GAL4-driven *gfp–smo* transgenic flies (*G,H*) with DIG-labeled ribo-probes: *smo* antisense probe (*E,H*), *smo* sense probe (*F*), and *gfp* antisense probe (*G*). (*I–N*) GFP (*I*) and GFP–Smo (*J–N*) expression in wing discs of flies expressing the indicated transgenes, all expressed using 71B–GAL4.

1B,C). A similar wing phenotype was observed when a stronger GAL4 driver, MS1096 was used (Supplementary Fig. 2D). The modest effect of Smo overproduction on development of wings may be attributable to posttranscriptional events that limit Smo activity through Ptc. Overproduction of Ptc or Ptc–YFP using 71B–GAL4 reduced wing size (Supplementary Fig. 1D; data not shown; Johnson et al. 1995). Overproduction of Ptc together with GFP–Smo did not change wing size or venation, suggesting that Ptc prevails over Smo (Supplementary Fig. 1E). When GFP–Smo, Ptc, and Hh were all overproduced, the wing size and venation appeared almost wild-type and the extra cross-vein was eliminated (Supplementary Fig. 1F). GFP–Smo and Ptc–YFP have activities similar to the untagged proteins.

Posttranscriptional regulation of GFP–Smo by Hh and Ptc

GFP–Smo is posttranscriptionally regulated by Hh and Ptc. *smo* transcript is ubiquitous (Fig. 1E; Alcedo et al. 2000; Denef et al. 2000; Ingham et al. 2000). In wing discs where 71B–GAL4 was used to produce extra *smo* RNA, *smo* and *gfp–smo* RNA look ubiquitous, though not even (Fig. 1G,H). Under these conditions GFP–Smo protein was at much higher levels in posterior regions of the disc, that is, in regions where Smo protein normally accumulates and where Hh is produced (Fig. 1J). Ectopic expression of *hh* in the anterior disc led to high-level accumulation of GFP–Smo in the anterior as well (Fig. 1K). Conversely, when *ptc* was coexpressed using the same 71B driver, GFP–Smo levels were reduced to approximately the level observed in the anterior of normal discs (Fig. 1L). When both *hh* and *ptc* were ectopically expressed, GFP–Smo levels were comparable with GFP–Smo in a wild-type background, but slightly lower (Fig. 1, cf. M and J).

Ptc1130X, a dominant-negative form of Ptc (PtcDN), activates Hh target gene transcription in the absence of Hh signal (Johnson et al. 2000). When *ptcDN* was expressed using 71B–GAL4, GFP–Smo levels were considerably higher in both the anterior and posterior compartments, indicating that the altered Ptc caused increased Smo accumulation in the anterior compartment as would be expected for a dominant-negative protein (Fig. 1N). Therefore, GFP–Smo, like Smo itself (Alcedo et al. 2000; Denef et al. 2000), is posttranscriptionally regulated, accumulating to higher levels in cells that produce or receive Hh signal. Smo protein levels are lower in cells where Ptc is produced. Because the transgenes contained the *smo* protein-coding sequence, but not 5′ or 3′ untranslated sequences, the posttranscriptional regulation of Smo is likely to be posttranslational.

Hedgehog signaling in salivary gland cells

The small size of embryonic and imaginal disc cells makes observing protein localization difficult. To examine the subcellular location of Smo protein we used early third instar larval salivary gland cells that have a volume several hundred times larger than most other fly cells (Andrew et al. 2000). In situ hybridizations show that normal salivary gland cells have *hh*, *smo*, and *ptc* transcripts present (Fig. 2G–K; data not shown).

We tested whether salivary gland cells are responsive to Hh signal (driven by a heat-shock promoter, *hs–hh*) using a *ptc–lacZ* target gene that responds to Hh in many other cell types (Ingham and Fietz 1995). In salivary glands with no added *hh* expression, a low level of *ptc–lacZ* expression was detected with X-Gal staining (data not shown). The level was similar in non-heat-shocked flies carrying the *ptc–lacZ* and *hs–hh* transgenes (Fig. 2B). After a heat shock to provide increased Hh protein, the *hh* and *ptc* RNA levels were higher (Fig. 2G–I; data not shown), and the level of *ptc–lacZ* expression was similarly elevated (Fig. 2C). To measure induction accurately, protein extracts were prepared from wild-type, non-heat-shocked, and heat-shocked glands and the level of β-galactosidase activity was measured, normalized to the amount of protein in each extract. The added Hh protein caused an ~13-fold increase in β-galactosidase activity. There were no changes in luciferase activity, which served as an internal negative control (Fig. 2D).

Ptc represses its own transcription in Hh-responsive tissues. Full-length Ptc was produced in salivary glands using 71B–GAL4, which drives UAS transgenes in salivary glands as well as in imaginal discs. The expression of *ptc–lacZ* was reduced to the basal level (Fig. 2E). In contrast, the dominant-negative form of *ptc*, *ptcDN*, strongly induced *ptc–lacZ* expression (Fig. 2F). These results indicate that salivary gland cells respond to the Hh signal and to Ptc.

Movement of Smo to the cell surface in response to Hh signaling

The ability of salivary gland cells to respond to Hh allowed an examination of GFP–Smo localization in gland cells, with or without added Hh protein. GFP, GFP–Smo, and other proteins were produced in salivary glands using 71B–GAL4, which drives expression ubiquitously in the glands (e.g., see Fig. 2L). Cell nuclei were marked with a red dye, 7AAD (arrow, Fig. 3A). GFP was present in both cytoplasm and nuclei in gland cells with or without added Hh (Fig. 3A,B). Expression of Hh had no obvious effect on salivary gland morphology (Fig. 2B,C; data not shown). Without added Hh, low amounts of GFP–Smo were located in a network of intracellular structures (arrow, Fig. 3C). Salivary gland cells contain globules of saliva that exclude GFP–Smo; GFP–Smo is also not detected in nuclei. Relative fluorescence intensities were measured using MetaMorph software. Without added Hh, the surface versus intracellular GFP–Smo ratio was 2:9. In salivary glands where HhN (an active form of Hh signal) was produced, GFP–Smo underwent a dramatic shift to the cell surface (arrow, Fig. 3D). The fluorescence intensity of surface versus intracellular GFP–Smo in-

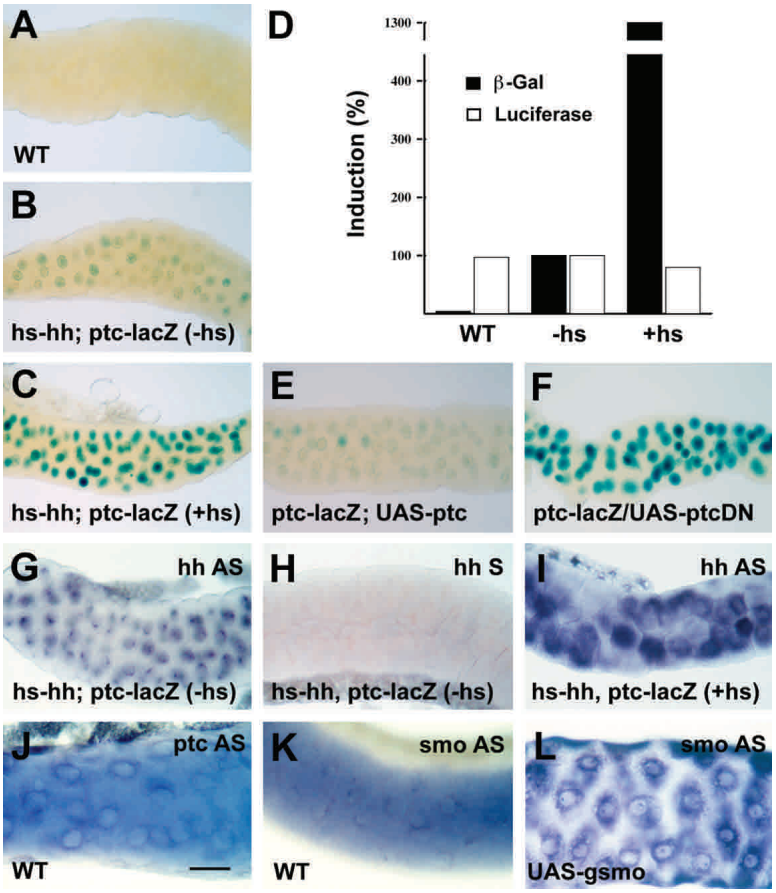

Figure 2. Salivary gland cells are responsive to Hh signal. (*A–C,E,F*) X-Gal staining of salivary glands from wild-type (*A*), *ptc–lacZ* transgenic flies without Hh (*B*), with Hh provided by the heat-shock (hs) promoter (*C*), with *ptc* (*E*), or with a dominant-negative *ptc* transgene (*F*) driven by 71B–GAL4. Bar, 200 μm. (*D*) Comparison of β-galactosidase levels in salivary glands from wild-type (WT), *ptc-lacZ* transgenic flies without Hh (–hs) or with Hh provided by the heat-shock promoter (+hs). Luciferase activity served as a loading control. Solid bars indicate β-galactosidase activity; open bars indicate luciferase activity. Percent induction of both activities was shown on the *Y*-axis. Percentage induction in *D* was from a typical experiment. (*G–L*) In situ hybridization of salivary glands from *hs–hh; ptc–lacZ* flies without Hh (*G,H*) or with Hh provided by the heat-shock promoter (*I*), wild-type flies (*J,K*), or *gfp–smo* flies driven by 71B–GAL4 (*L*). (*G,I*) *hh* antisense probe. (*H*) *hh* sense probe. (*J*) *ptc* antisense probe. (*K,L*) *smo* antisense probe. Bar, 100 μm.

creased from 2:9 for the control to 7:3. The area counted as surface was ~5%–10% of the entire area, so the density of GFP–Smo fluorescence at the surface is 20× the average density internally.

The movement of GFP–Smo to the cell surface was also observed in *Drosophila* embryos and cultured cells, in keeping with previous observations of untagged Smo in wing discs (Denef et al. 2000). *gfp–smo* and *hhN* were coexpressed in embryos using *en*–GAL4 and a similar Hh-induced change in location was seen (arrow, Supplementary Fig. 3C). GFP–Smo, produced in cultured *Drosophila* imaginal disc cl-8 cells, moved to the cell surface when cells were incubated in conditioned medium from S2 cells producing HhN (arrow, Supplementary Fig. 3E), whereas GFP–Smo remained in the intracellular compartments when control S2 medium was added to the cells (Supplementary Fig. 3D). Little or no change in the total strength of the GFP signal occurred as a consequence of HhN overexpression in gland cells, embryos, or cl-8 cells (data not shown). The movement of GFP–Smo from internal compartments of salivary gland cells is consistent with the observation that GFP–Smo, and endogenous Smo, is posttranscriptionally regulated in wing imaginal discs. Smo protein is at a lower level and may rapidly turn over in the anterior half of the disc, away from the Hh source.

To examine the behavior of Ptc in large salivary gland cells a *ptc–yfp* construct (*ptcy*) was expressed using 71B–GAL4. Ptc–YFP protein accumulated to levels higher than those of GFP–Smo in salivary gland cells in a punctate pattern decorating a network of intracellular structures, and also in perinuclear regions (Fig. 3E). On Hh production in salivary glands, Ptc–YFP underwent a dramatic change. Ptc–YFP protein was no longer detected in the plasma membrane and instead became concentrated in perinuclear regions (arrow, Fig. 3F). Therefore, in salivary glands, Hh causes internalization of Ptc protein as it does in imaginal disc cells (Denef et al. 2000). We cannot monitor GFP–Smo and Ptc–YFP simultaneously as it is not possible to distinguish GFP from YFP. The movements of GFP–Smo and Ptc–YFP are strikingly different, so the Hh-induced changes are not a general movement of membrane proteins to one destination.

The dominant-negative form of Ptc (PtcDN) activates Hh target gene transcription in the absence of Hh signal (Johnson et al. 2000). To examine the localization of PtcDN, a *ptcDN–yfp* construct (*ptcDNy*) was expressed in salivary gland cells using 71B–GAL4. PtcDN–YFP protein had a distinctive localization pattern; it accumulated strongly in a discontinuous, dotted pattern along the plasma membrane (Fig. 3G). YFP tagging was compatible with the function of both Ptc and PtcDN. Overproduction of Ptc–YFP in adult wing led to loss of the wing tissue between L2 and L4, the same effect as Ptc

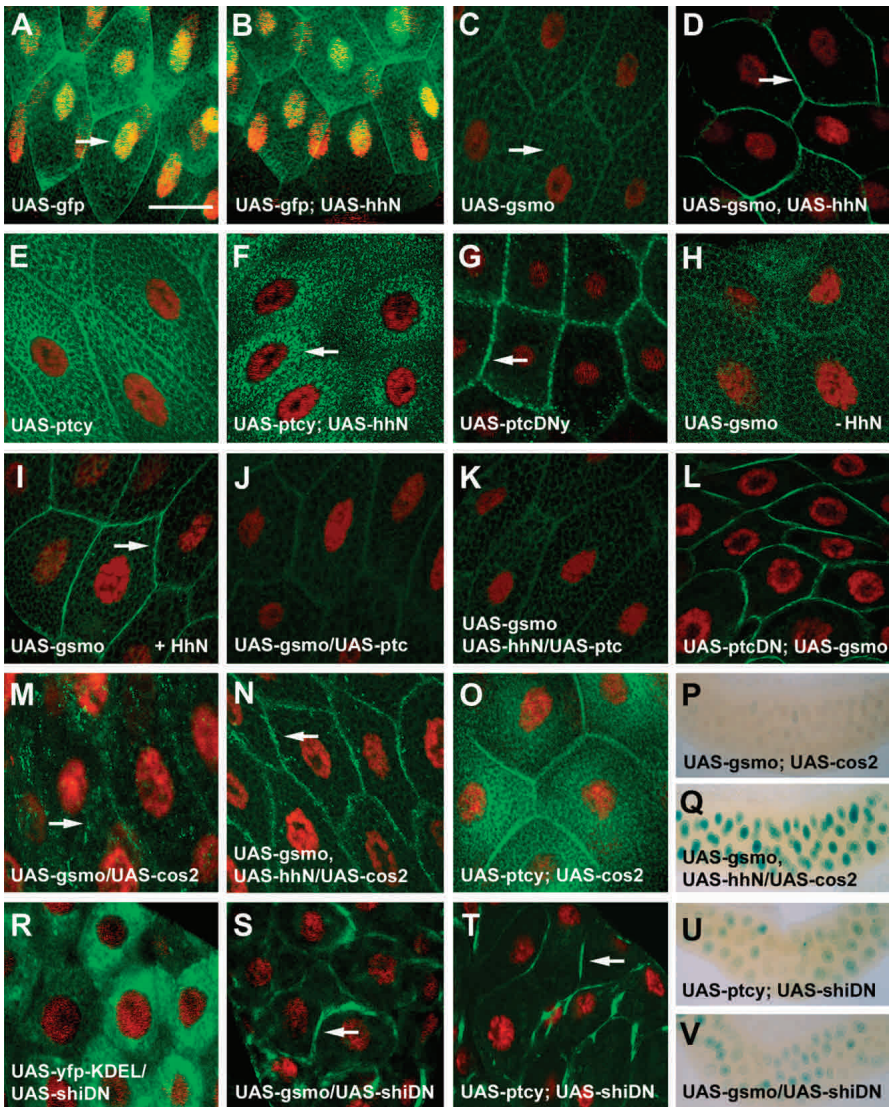

Figure 3. Movement of Smo to the cell surface in response to Hh signaling. (*A–O,R–T*) Salivary glands from different transgenic flies were dissected and fixed in paraformaldehyde. The *gfp* (*A,B*), *gfp–smo* (*C,D,H–N,S*), *ptc–yfp* (*E,F,O,T*), *ptcDN–yfp* (*G*), and *yfp–KDEL* (*R*) expression pattern (green) was examined using confocal microscopy. Cell nuclei were labeled with 7AAD (red). Arrows indicate nuclei (*A*), internal membrane compartments (*C,M*), plasma membrane (*D,G,I,N,S,T*), and perinuclear region (*F*), respectively. Bar, 50 μm. (*P,Q,U,V*) X-Gal staining of salivary glands from flies expressing *ptc–lacZ*, *gfp–smo*, and *cos2* without (*P*) or with (*Q*) *hhN*, or *ptc–lacZ*, dominant-negative *shi* together with *ptc–yfp* (*U*), or *gfp–smo* (*V*) using 71B–GAL4. Bar, 300 μm.

alone (Johnson et al. 1995). In contrast, PtcDN–YFP, like PtcDN (Johnson et al. 2000), increased venation and the size of the adult wings (data not shown).

To determine the kinetics of the response of GFP–Smo to Hh, salivary glands carrying the transgene were put into culture. GFP–Smo was visible in intracellular membranous compartments after 24 h in culture (Fig. 3H; data not shown). When recombinant HhN protein was added to the culture, GFP–Smo moved to the salivary gland cell surface within 30 min (arrow, Fig. 3I). There was no apparent difference in GFP–Smo movement when a modified HhN, OS-7 [HhN peptide modified by addition of a hydrophobic eight-carbon chain (octyl-group) to the N-terminal cysteine] or the concentrated conditioned medium from S2 cells producing HhN was added in culture (data not shown).

Regulators of Hh target gene transcription control Smo location

The movement of GFP–Smo to the surface of salivary gland cells in response to Hh was used as an assay to learn how other Hh pathway regulators affect Smo localization. Overexpression of *ptc* alone in salivary gland cells using 71B–GAL4 had no obvious effect on GFP–Smo localization (Fig. 3J). Overproduction of Ptc along with HhN blocked most of the movement of Smo to the cell surface (Fig. 3K). The dominant-negative form of Ptc

(PtcDN) had the opposite effect. An intense GFP–Smo signal was observed at the cell surface even without added Hh (Fig. 3L). These results indicate that a normal function of Ptc is to confine Smo to internal cell locations.

Costal2 (Cos2) is a kinesin-related protein that negatively regulates transcription of Hh target genes (Robbins et al. 1997; Sisson et al. 1997), evidently as a member of an intracellular protein complex (Stegman et al. 2000). Cos2 has been thought to operate downstream of Smo in controlling Hh signal transduction (Nybakken and Perrimon 2002). Overexpression of *cos2* eliminates Hh target gene expression (Fig. 3P) and causes smaller wing size with some wing vein tissue missing (K.S. Ho and M.P. Scott, unpubl.). Cos2, however, a putative microtubule-based motor, can affect Smo localization. Overexpression of *cos2* in salivary gland cells using 71B–GAL4 decreased Hh target gene activation (Fig. 3P) and caused GFP–Smo to move to discreet internal locations (Fig. 3M). In addition, overexpression of *cos2* in combination with Hh allowed GFP–Smo to move to the surface, but GFP–Smo did not accumulate in its normal solid pattern at the cell surface. Instead, a punctate GFP–Smo signal is observed along the plasma membrane (arrow, Fig. 3N). In this situation, *ptc–lacZ* was moderately activated (Fig. 3Q) so the Cos2 blocks to some degree the effect of Hh. Overexpression of a different kinesin-related protein, Nod (fused to β-galactosidase and still functional; Clark et al. 1997), had no detectable effect on GFP–Smo localization with or without Hh present (data not shown). In contrast, *cos2* overproduction had little effect on Ptc–YFP localization in salivary gland cells (Fig. 3O); this combination of regulators (Cos2 and Ptc–YFP) did not activate *ptc–lacZ* target gene transcription (data not shown).

The consequences of protein synthesis, phosphorylation, cytoskeletal structure, and endocytosis for Smo relocation

To test whether the translocation of Smo from the intracellular compartments to the cell surface was dependent on continuing protein synthesis, we treated cultured salivary glands with cycloheximide for 1–2 h at 25°C before adding HhN. GFP–Smo moved to the cell surface despite the protein synthesis block (Supplementary Fig. 4A), although the overall intensity was somewhat lower than in controls treated with HhN alone (data not shown). The appearance of Smo at the surface is largely movement of protein rather than new synthesis.

Experiments with cultured *Drosophila* wing disc cells suggested that phosphorylation stabilizes Smo protein at the cell surface, even without Hh activation (Denef et al. 2000). We treated salivary gland cells with either of two phosphatase inhibitors—calyculin A (inhibiting both tyrosine and serine/threonine protein phosphatases) and okadaic acid (specific for serine/threonine protein phosphatase). Smo–GFP protein was more highly phosphorylated after the addition of either inhibitor as examined in SDS-PAGE followed by Western blotting with a rabbit anti-GFP polyclonal antibody AB3080 (data not shown). After inhibitor treatment, little if any Smo protein accumulates at the cell surface (Supplementary Fig. 4B; data not shown). Blocking phosphatase activity is not sufficient to cause Smo to become enriched at the surface.

Because Cos2, a kinesin-related protein, affected Smo protein subcellular localization, we tested whether the tubulin or actin cytoskeleton is involved in Smo protein translocalization. Before adding recombinant HhN protein, salivary gland cells were incubated with nocodazole, a drug that largely destroys the tubulin network, or latrunculin A, an actin cytoskeleton inhibitor. With the addition of either drug, Smo proteins remained largely in intracellular compartments despite HhN treatment (Supplementary Fig. 4E,I). To confirm the elimination of the cytoskeletal structures, salivary gland cells were immunolabeled with antibodies to tubulin or actin (Supplementary Fig. 4D,H). After nocodazole treatment, the tubulin networks were abolished and after latrunculin A, no actin cytoskeleton remained (Supplementary Fig. 4F,J). Both the actin cytoskeleton and the tubulin networks are required for moving Smo protein from cytoplasmic compartments to the cell surface.

Smo protein appears to cycle continuously between internal vesicles and the plasma membrane (Martín et al. 2001; Strutt et al. 2001; Incardona et al. 2002), a process that may require endocytosis. Dynamin is essential for receptor-mediated endocytosis. *shibire* (*shi*) encodes the fly dynamin homolog (van der Bliek et al. 1993). A dominant-negative form of Shi, ShiK44A (ShiDN), fails to bind or hydrolyze GTP, and blocks clathrin-coated vesicle formation when overexpressed in cultured cells and fly embryos (van der Bliek et al. 1993; Moline et al. 1999). We tested whether disruption of endocytosis has any effect on Smo relocation using a UAS–*shiDN* transgene driven by 71B–GAL4. Without Hh stimulation, GFP–Smo normally resided in internal organelles of salivary gland cells (Fig. 3C), whereas Ptc–YFP was divided between internal and surface locations (Fig. 3E). When endocytosis was disrupted by ShiDN, both GFP–Smo and Ptc–YFP accumulated at the cell surface (arrows, Fig. 3S,T). When *shiDN* was expressed, the surface-localized GFP–Smo did not activate *ptc–lacZ* expression (Fig. 3, cf. V and U), perhaps because of the simultaneous presence of endogenous Ptc at the cell surface. In contrast, ShiDN has little effect on YFP protein trapped in the ER (YFP fused with a C-terminal KDEL tag; YFP–KDEL; Fig. 3R). The KDEL motif functions as an ER retrieval signal for ER resident proteins (Munro and Pelham 1987).

The dynamin experiment suggested that Smo might move through the endocytic pathway, in which case *Rab5* and *Rab7* mutants might affect Smo localization. The small GTPase Rab5 has a role in the formation of clathrin-coated pits and their subsequent fusion with early endosomes (Bucci et al. 1992; McLauchlan et al. 1998), whereas Rab7 is essential for transporting endocytic cargos from the early to the late endosome and lysosome (Vitelli et al. 1997). Like their mammalian counterparts, fly Rab5 and Rab7 accumulate in early and

late endosomal structures, respectively (Entchev et al. 2000).

We overexpressed dominant-negative Rab5 (Rab5S43N; Entchev et al. 2000) together with GFP–Smo in salivary gland cells. GFP–Smo accumulated at the cell surface even in the absence of added Hh (Supplementary Fig. 5A), a phenotype that is similar to that of overexpression of *shiDN*. In contrast, a dominant gain-of-function *Rab7* mutant (Rab7Q67L; Entchev et al. 2000) enhanced internalization and degradation of Smo protein (Supplementary Fig. 5B). In agreement with the dominant-negative *shi* results, overexpression of Rab proteins did not activate *ptc–lacZ* gene expression (Supplementary Fig. 5C–E). Taken together, relocation and degradation of Smo and possibly Ptc appear to be dependent on endocytic regulation.

Surface localization of Smo mutants related to oncogenic human alleles

Hh causes Smo to accumulate at the cell surface, but is the presence of Smo at the surface important for Hh signal transduction? To see if Smo activity correlates with surface localization in other circumstances, we examined the localization of an inappropriately active Smo mutant. Two oncogenic versions of Smo were discovered in humans afflicted with basal cell carcinoma (Xie et al. 1998). The activated forms differ by single amino acid changes in the putative transmembrane helix (M2) and in the region immediately following (M1). The amino acids at the sites of mutation are highly conserved among the Smo proteins of different species. We built each of the two mutations into a fly *gfp–smo* transgene and expressed the genes in flies. Production of either mutant Smo form (M1 or M2), using 71B–GAL4 caused stronger and qualitatively different changes in wing morphology compared with wild-type Smo (Supplementary Fig. 2A,B). When a stronger wing imaginal disc driver, MS1096–GAL4, was used to express either mutant form, overgrowth was seen in anterior adult wings (arrows, Supplementary Fig. 2E,F); this was never seen with wild-type Smo (see Supplementary Fig. 2D). The mutant GFP–Smo proteins accumulated at equally high levels in the anterior and posterior halves of wing discs (Fig. 4A,C), in contrast to GFP–Smo (Fig. 1J). Both mutant proteins

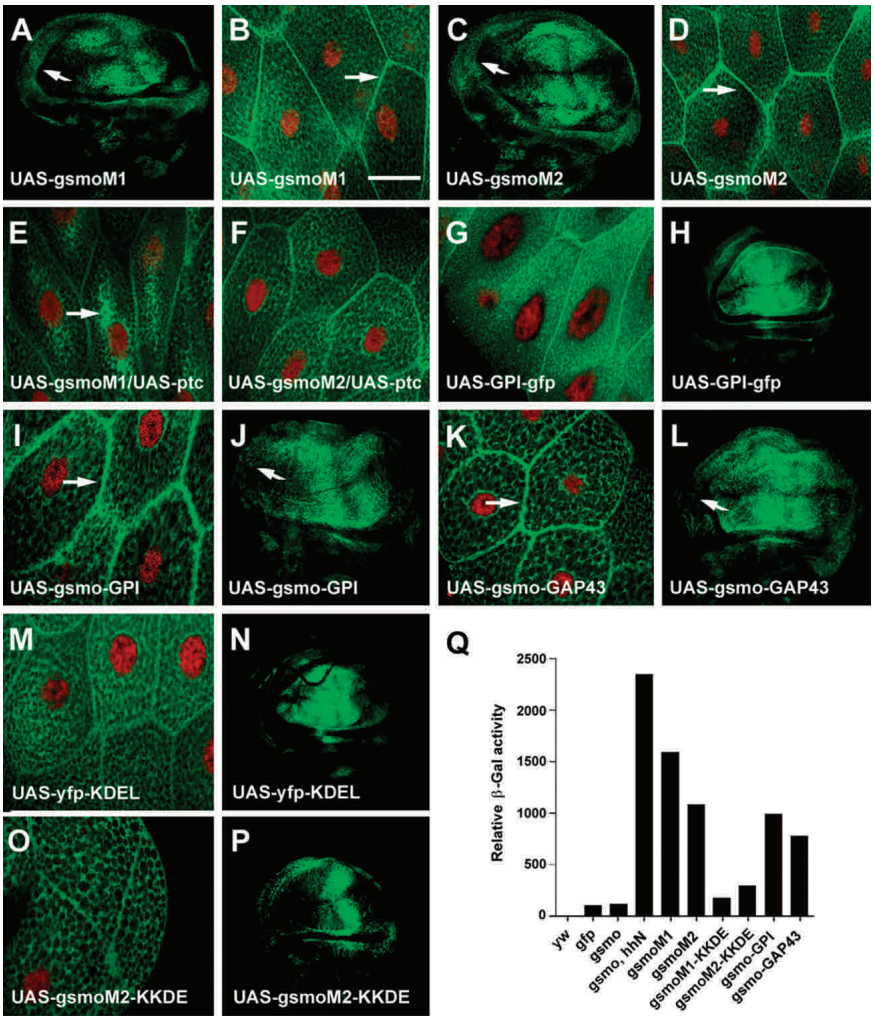

Figure 4. Biological effects of Smo mutants designed to alter intracellular protein localization. (*A*,*C*,*H*,*J*,*L*,*N*,*P*) GFP–SmoM1 (*A*), GFP–SmoM2 (*C*), GPI–GFP (*H*), GFP–Smo-GPI (*J*), GFP–Smo–GAP43 (*L*), YFP–KDEL (*N*), and GFP–SmoM2–KKDE (*P*) protein expression in wing imaginal discs of flies expressing transgenes as shown using 71B–GAL4. Note equal levels of active Smo (SmoM1 and SmoM2) in both anterior and posterior compartments of wing discs. Arrows indicate the overgrowth of the anterior side of the discs (*A*,*C*). (*B*,*D*,*E–G*,*I*,*K*,*M*,*O*) Salivary glands from transgenic flies, as shown, were dissected and fixed. GFP–Smo localization (green) and cell nuclei (labeled with 7AAD, red) were imaged with confocal microscopy. Arrows indicate plasma membrane localization (*B*,*D*,*I*,*K*) and the cytoplasmic accumulation of Smo (*E*). Bar, 50 µm. (*Q*) Comparison of β-galactosidase levels of salivary glands from wild-type flies (yw), transgenic flies expressing *gfp*, *gfp–smo*, *gfp–smo* together with *hhN*, and various *gfp–smo* mutant transgenes, using 71B–GAL4. Percent induction of β-galactosidase activity was shown on the *Y*-axis. Relative activity in *Q* was from a typical experiment. The protein concentrations of the GFP–Smo fusions were compared by Western analysis with a rabbit polyclonal anti-GFP antibody (see Supplementary Fig. 7).

caused anterior disc overgrowth (indicated by arrows in Fig. 4A,C).

The mutant fly Smo proteins have an altered subcellular location. Even without adding Hh, both mutant forms of the protein accumulated extensively at the surfaces of salivary gland cells (arrows, Fig. 4B,D). The fluorescence intensity of surface versus intracellular GFP–SmoM1 ratio was 2:3, whereas the surface versus intracellular GFP–SmoM2 ratio was 1:1. There was no further increase in surface localization when UAS–*hhN* was coexpressed (data not shown). The mutations may therefore affect a part of the Smo protein necessary for its containment in internal organelles, an internalization that is driven at least in part by Ptc. In the absence of added Hh, overexpression of fly *ptc* lessened the fraction of mutant Smo that accumulated at the surface (Fig. 4E,F); Ptc affected M1 more than M2. The mutant proteins may be more resistant to Ptc-driven internalization than the wild-type protein, but not completely resistant.

Biological effects of Smo mutants designed to alter intracellular protein localization

We altered Smo with two types of membrane localization signals that are commonly used for targeting protein fusions to the cell surface. One is the glycosylphosphatidylinositol (GPI) anchor (Benting et al. 1999) that targets proteins to the outer face of the lipid bilayer; the other is the N-terminal 20 amino acids of neuromodulin (GAP43; Strittmatter et al. 1994) that anchor proteins at the inner membrane through palmitoyl groups attached to a pair of Cys residues. We constructed transgenes coding for either a GPI or a GAP43 tag at the C terminus of GFP–Smo, and expressed the transgenes in flies using 71B–GAL4. Both GPI and GAP43 brought GFP–Smo to the surfaces of salivary gland cells (arrows, Fig. 4I,K).

Overproduction of either membrane-anchored GFP–Smo, using MS1096–GAL4, causes a stronger adult wing phenotype than overexpression of *smo*. Overgrowth of wing discs (arrows, Fig. 4J,L) and of anterior wing (arrows, Supplementary Fig. 2I,J) was clear with both mutant proteins, a phenotype similar to that resulting from overexpression of activated *smo* mutants. The membrane-anchored Smo proteins were produced at equally high levels in the anterior and posterior compartments of wing imaginal discs (Fig. 4J,L), and are therefore resistant to whatever process normally destabilizes Smo protein in the anterior compartment. A GFP transgene with a GPI anchor did not have any effect on wing imaginal discs or morphology of adult wing (Fig. 4H; data not shown).

Surface location of Smo correlates well with Hh target gene transcription. We tested the effect of preventing Smo from leaving the ER. Many ER resident, membrane-bound proteins contain a KKXX (Lys-Lys-X-X) motif at the C terminus. They are exported into the *cis*-Golgi network like other membrane proteins. The KKXX-containing proteins then interact directly with COPI coats and are packaged into COPI-coated vesicles for retrograde delivery to ER (Lotti et al. 1999). We created a KKDE motif at the C terminus of each activated form of Smo (GFP–SmoM1–KKDE and GFP–SmoM2–KKDE). As a control, we produced YFP protein fused with the KDEL motif (YFP–KDEL) in salivary gland cells (Fig. 4M).

The M1 and M2 Smo–KKDE fusions were largely absent from the cell surface of the salivary gland cells (Fig. 4O; data not shown). Instead they were located in intracellular compartments containing the protein disulfide isomerase (PDI), which is an abundant component of the ER (McKay et al. 1995; Supplementary Fig. 6; data not shown). The levels of overproduced, activated M1 and M2 Smo–KKDE fusions were much lower in anterior wing discs, like Smo–GFP but unlike M1 or M2, and the disc size was normal (Fig. 4P; cf. Figs. 1J and 4A,C). Only a very subtle wing phenotype was observed when either KKDE-tagged M1 or M2 Smo was expressed using MS1096-GAL4 (Supplementary Fig. 2G,H). The KKDE-tagged activating Smo mutants were not able to cause any obvious defects in wing imaginal discs. The activation of Smo that occurs because of the M1 and M2 mutations is therefore eliminated by adding three amino acids to the normal C-terminal "K."

To compare levels of Hh target gene expression stimulated by the different modified Smo constructs, protein extracts were prepared from flies carrying a *ptc–lacZ* reporter in combination with different *gfp–smo* transgenes, and the level of β-galactosidase activity in salivary gland extracts was measured. The activity was normalized to the amount of protein in the extracts based on protein blotting. GFP antibody was used to detect tagged Smo proteins and β tubulin antibody was used as a loading control. No free GFP (~30 kD) was detected on protein blots; the GFP tag remained attached to Smo (Supplementary Fig. 7). Very low-level β-galactosidase activity was observed in extracts from flies expressing *gfp* or *gfp–smo* (Fig. 4Q). The addition of Hh protein caused an ~20-fold increase in β-galactosidase activity. Smo activating mutations and GPI signal- or GAP43-tagged Smo had β-galactosidase activity that was ~7- to 13-fold higher than the GFP–Smo control. Adding a KKDE tag to the activated Smo forms brought β-galactosidase activity back down to that of GFP–Smo (Fig. 4Q).

Together, the results indicate a strong correlation between cell surface localization and heightened Smo activity. Smo accumulates at the cell surface (1) in response to Hh, (2) when Ptc function is reduced, and (3) when activated forms of Smo are produced. Preventing cell surface localization of activated forms of Smo by adding an ER retrieval motif reduces Hh activation. Altered forms of Smo that move to the surface are able to activate Hh target gene transcription, stimulate anterior growth of imaginal discs, and alter wing morphology.

Discussion

Surface Smo localization and Hh target gene activation

The salivary gland experiments show that Smo is normally present in a meshwork of organelles in the cyto-

plasm. On reception of a Hh signal, Smo protein moves quickly to the surface. This occurs within 30 min and is not dependent on protein synthesis, so the change is in fact movement and not turnover followed by new synthesis. Such a change in subcellular localization could be attributable to release from a tether and movement, or to a change in the net flow of protein cycling through membrane compartments. If Smo, for example, normally circulates to and from the surface (Kalderon 2000), Ptc could facilitate the inward movement. When Hh binds to Ptc and inactivates it, Smo would cycle to the surface and remain there. This idea is consistent with the increased surface Smo observed when endocytosis is blocked with the *shibire* or *Rab5* mutation.

Surface Smo localization correlates fully with Hh target gene transcription but the amount of Smo protein does not. The apparent increase in the amount of Smo at the cell surface that occurs when Hh signal is received may be caused by sequestration of Smo away from proteases in internal membrane compartments. Smo moves to the surface on addition of Hh or removal of Ptc, conditions that activate target gene transcription.

The mutant forms of fly Smo designed to mimic human oncogenic *SMO* alleles (Xie et al. 1998) were also located at the surface. The basis for the tumors is hypothesized to be inappropriate activation of Hh (perhaps Shh) target genes in the skin and cerebellum, targets that are insufficiently restrained by Ptc1 or other regulators. The oncogenic forms of Smo appear to be resistant to inhibition by Ptc and at least one of them is clearly resistant to teratogenic drugs that bind Smo and inhibit responses to Hh signaling (Taipale et al. 2000; Chen et al. 2002). Our experiments suggest that the fly versions of the oncogenic proteins are also at least partially resistant to Ptc and are refractory to the Ptc-imposed internalization of Smo protein. Overexpression of the oncogenic mutants causes dramatic changes in wing patterning and anterior outgrowth. Conversely, tagging oncogenic Smo mutants with an ER retrieval motif, KKDE at the C terminus prevents Hh signaling. This addition of only three amino acids (one K is already present at the C terminus of fly Smo) drastically changed the activities and localization of the protein.

Forms of Smo with surface localization signals added at the C terminus are in fact enriched at the cell surface and these proteins activate Hh target gene transcription. These results suggest the importance of subcellular localization for regulating Smo activity. Smo normally resides in internal compartments of unknown character, and moves in response to Hh and other regulators. We cannot know whether it is surface localization per se that is important, or instead a movement to new compartments that happen to locate at or near the cell periphery.

Smo protein is predicted to have seven transmembrane domains. The C terminus of Smo protein, where the GAP43 and GPI linkage sequences were added, is predicted by most modeling programs to be cytoplasmic, but given the absence of any data on the actual transmembrane topology of Smo, two tags with different properties were used. The GAP43 tether works from the cytosolic side (Resh 1999), whereas the GPI tether is believed to work only if the tagged part of the protein is on the luminal side of the membrane (Muñiz and Riezman 2000).

The successful activation of Smo by the GAP43 tether is consistent with the presumed topology. This topology would mean, however, that the GPI tether is not formed because the necessary machinery to cleave the GPI signal is located in the lumen of the ER. The appearance of the surface-localized Smo differs for the two tags (Fig. 4I,K), with the GPI-motif protein giving a continuous pattern that connects adjacent cells and the GAP43 sequence giving discernably separate layers of protein on two adjacent cells. Two possible explanations of the GPI results are that the tag alters the Smo protein topology so that the protein becomes GPI-linked or that the tag changes Smo conformation to make an activated molecule (cf. Lu et al. 2002). Taipale et al. (2000) proposed that Smo cycles between two different conformations. The movement of Smo to a new location might shift the balance toward the active state of Smo, for example if the pH, ionic milieu, lipid composition, or presence of other proteins in the new compartment alter Smo conformation. The GPI signal could alter the Smo conformation to an active form, and in this case surface localization could be a consequence, rather than cause, of activation.

Inhibition of Smo function by Ptc

Flies lacking *smo* function are unable to activate target genes in response to Hh signaling, in contrast to *ptc* mutants, which activate target genes inappropriately even in the absence of Hh signal. Double mutants that lack both *smo* and *ptc* function fail to activate Hh target gene transcription, indicating that the failure of repression by Ptc is irrelevant if Smo is not present to allow activation (Forbes et al. 1993). On this basis, Ptc has been viewed as an opponent of Smo function.

Smo is similar to the Frizzled (Fz) Wnt receptors in primary sequence and presumed structure, but Smo has no known ligand and as yet has not been found to bind a Wnt protein (R. Nusse, pers. comm.). Surface localization could be critical if it allows an as-yet-unknown activating ligand to bind Smo. A limiting amount of ligand might explain why over-producing Smo alone does not have a strong effect on development.

The regulation of Smo by Ptc remains a mystery. Hh could inactivate Ptc by binding to it either on the surface or in internal vesicles (Incardona et al. 2002). If Ptc cycles between surface and interior regions of the cell, the binding by Hh could change Ptc so that it is less likely to travel to the surface. In contrast to Hh inactivation of Ptc, mutational inactivation of Ptc does not lead to an internal location, at least in the case of the dominant-negative form that accumulates at the surface. Ptc, possibly through a transporter function (Ioannou 2001; Taipale et al. 2002), could change organelle contents or composition so that Smo changes conformation to its active form. Alternatively Ptc could either detach Smo

from an intracellular tether or alter the movements of vesicles bearing Smo protein. Smo, previously cycling to and from the surface, would accumulate on the surface and increase in amount.

Signaling from Smo, through a Gα protein or other means, could alter the cytoplasmic Ci complex and change Ci processing to control target gene transcription. Two experiments in frog melanophores and zebrafish embryos have suggested possible Gα(i) involvement in Hh signal transduction (Hammerschmidt and McMahon 1998; DeCamp et al. 2000). As both studies involved overexpression of proteins, it is unclear as yet whether Smo acts through G protein signal transduction. An alternative, more direct interaction with the cytoplasmic protein complex seems possible, for example, if Smo controls encounters between the complex and the as-yet-unknown protease that cleaves Ci.

The dominant-negative form of Ptc is present at the cell surface and could compete for an association between Ptc and Smo, compete for an association between Ptc and another protein, or associate with wild-type Ptc and inactivate its activity. The distinct locations of Ptc and Smo in fly imaginal disc cells (Denef et al. 2000) and, as shown here, in salivary gland cells, suggest that the bulk of each protein is not in association with the other protein. There could nonetheless be some of the proteins in association, below the level of detection by staining techniques. Although little or no Ptc–Smo association was seen by immunoprecipitation from cultured cells (Johnson et al. 2000; Incardona et al. 2002; Taipale et al. 2002), transient associations would not be seen, particularly if the arrival of Ptc or Hh/Ptc in a Smo-containing organelle immediately caused the departure of Smo (cf. Incardona et al. 2002).

Ptc contains a sequence related to "sterol-sensing domains (SSDs)" that have been implicated in altered functions or stability of proteins involved in lipid metabolism. Mutations in the Ptc SSD reduce the ability of Ptc to repress Smo function (Martín et al. 2001; Strutt et al. 2001). It is possible that Ptc regulates Hh signaling through effects on membrane trafficking. Analysis of mice with mutations in the *open brain* (*opb*) gene lent further support for the potential involvement of protein trafficking in Hh signal regulation. *opb* encodes Rab23, which negatively regulates Hh signal transduction (Eggenschwiler et al. 2001). Rab GTPases coordinate the budding, fission, transport, docking, and fusion of vesicles as they move from one cellular location to a target compartment (Somsel Rodman and Wandinger-Ness 2000). The shuttling of Smo and Ptc between internal membrane compartments and the cell surface presumably requires Rab activity. Disruption of endocytosis by dominant-negative Shibire and by Rab5 manipulation prevented both Smo and Ptc internalization.

Other regulators of Smo localization

Movement of Smo to the surface requires actin and tubulin components of the cytoskeleton, though the relevant motors are unknown. Cos2 is an unusual member of the kinesin family, with sequence features at odds with conventional ATPase binding site structure (Robbins et al. 1997; Sisson et al. 1997). Cos2 could be either a motor or a tether. Cos2 could have a role in controlling movements of vesicles that contain Smo. Overproduction of Cos2 altered GFP–Smo localization, and furthermore, prevented Hh from bringing much GFP–Smo to the surface, and the GFP–Smo that did reach the surface was located in discreet dots. Ptc also blocked Hh from bringing GFP–Smo to the surface, but no such dots were observed. Overexpression of a presumably irrelevant other motor protein, Nod (Clark et al. 1997), had no effect on localization of GFP–Smo. Cos2 production may therefore specifically cause the movement of Smo-containing organelles to discreet locations on the membrane, either tethering them to the cytoskeleton at specific locations or causing a coalescence effect at random locations. Cos2 has been envisioned as functioning as part of a cytoplasmic complex whose activity in processing the Ci transcription factor is controlled by Smo. The present data suggest a new function in which the complex, or Cos2 indepently of the complex, feeds back to alter Smo activity. It is interesting that both GFP–Smo (when Cos2 and Hh were coexpressed; Fig. 3N) and PtcDN–YFP (Fig. 3G) exhibited a similar punctate cell surface localization pattern. PtcDN may function through competing with endogenous Ptc (Johnson et al. 2000), raising an intriguing alternative possibility that Cos2 may interact directly with Smo to control Smo subcellular localization.

Human oncogenesis by activated Smo and the importance of the Hh pathway in numerous developmental events in all animals makes understanding Hh signal transduction critical. The present approach has identified new interactions between components of the pathway. The causal link between surface location and activity during Hh signaling, with Ptc inactivation, with Smo oncogenic mutants and with mislocalization of Smo add strong evidence that the localization of Smo is a critical regulatory step in Hh signaling.

Materials and methods

Fly strains and germline transformation

The following fly lines were used: *da*–GAL4, 71B–GAL4, MS1096–GAL4, *en*–GAL4, UAS–*ptcB1* (wild-type Ptc; Johnson et al. 1995), UAS–*ptc1130X* (dominant-negative Ptc; Johnson et al. 2000), H84 *ptc–lacZ*, *hs–hh* (wild-type Hh; Ingham and Fietz 1995), UAS–*hhN* (N terminus of Hh; Porter et al. 1995), UAS–*cos2* (Sisson et al. 1997), UAS–*nod–lacZ* (Nod fused to β-galactosidase; Clark et al. 1997), UAS–*gfp*, UAS–*GPI–gfp* (Greco et al. 2001), UAS–*shiK44A* (dominant-negative Shi; Moline et al. 1999), UAS–*Rab5S43N* (dominant-negative Rab5), and UAS–*Rab7Q67L* (dominant gain-of-function Rab7; Entchev et al. 2000).

The gene for the GFP (Clontech) tag was inserted in-frame after the Smo signal peptide coding sequence (after Ser 33). To generate surface-localized GFP–Smo, polynucleotides encoding the GAP43 N-terminal peptide (MLCCMRRTKQVEKNDED QKI) and the GPI peptide (LEETTPNKGSGTTSGTTRLLSGH TCFTLTGLLGTLVTMGLLT) were fused in-frame to the C-ter-

minal of GFP–Smo, respectively. Activated forms of fly Smo–M1 and M2 [corresponding to the human oncogenic versions M1 (Arg 580 to Gln) and M2 (Trp 553 to Leu); Xie et al. 1998] were created by site-directed mutagenesis (Stratagene) based on the *gfp–smo* construct. The ER localized GFP–SmoM1 and M2 were constructed by building an ER retrieval peptide, KKDE, onto the C terminus of activated Smo. The first "K" is part of the normal Smo sequence, so the coding sequence for only three amino acids was actually added. The gene for the yellow fluorescent protein (YFP) tag was fused to the C termini of fly Ptc and Ptc1130X. The ER-localized YFP construct, *yfp–KDEL*, was purchased from Clontech. The gene fusions were cloned into pUAST transformation vector. Transgenic *Drosophila* lines were established as described in Johnson et al. (1995). For each construct, multiple lines that carried the P element were recovered and analyzed.

Preparation of wings and cuticle preparation

All UAS–*gfp* and UAS–*yfp* stocks were balanced and crossed either to 71B–GAL4 or MS1096–GAL4 to obtain expression in wing imaginal discs and salivary glands, or to *en*–GAL4 for expression in embryos. Wings were dissected from adults and mounted as described (Johnson et al. 1995). For rescue experiments, smo^3, UAS–*gfp*/smo^3; *da*–GAL4 embryos, smo^3; UAS–*smo*/smo^3; *da*–GAL4 embryos and smo^3; UAS–*gfp–smo*/smo^3; *da*–GAL4 embryos were collected and aged at 18°C for 40 h and cuticles were prepared as described previously (Quirk et al. 1997).

Manipulations of wing imaginal discs and embryos

All fly crosses were done at 25°C except when mentioned otherwise. Wing imaginal discs were dissected from early wandering third-instar larvae (i.e., those that will pupariate in 12–24 h) of wild-type or transgenic flies expressing *gfp* constructs. RNA in situ hybridization was performed for *gfp*, *hh*, *ptc*, and *smo* as described (Johnson et al. 1995). For observing GFP–Smo, wing imaginal discs were fixed in 4% paraformaldehyde on ice for 12 min, quenched in 50 mM NH_4Cl, mounted in Fluoromount G (Southern Biotech), and examined with a Bio-Rad confocal microscope.

To immunohistochemically label GFP-tagged proteins, embryos producing GFP fusions were dechorionated, fixed in heptane/formaldehyde, and devitellinized with methanol. Embryos were then incubated with a mouse monoclonal anti-GFP antibody 3E6 (Quantum Bio) and the signal was amplified with a biotin-conjugated secondary antibody before developing the signal with DAB (Vector Lab).

Salivary glands and drug treatment

For *lacZ* induction experiments, early wandering third-instar larvae were heat shocked at 37°C for 30 min, allowed to recover at room temperature for 20 min, heat shocked again for 30 min, and allowed to recover for 20 min before dissection. Salivary glands were fixed in 1% glutaraldehyde and X-Gal staining was performed overnight at 37°C (Ingham and Fietz 1995). For the quantitative β-galactosidase activity assay, 40 pairs of salivary glands from wild-type flies and *ptc–lacZ* flies, with or without Hh provided by heat shock, were dissected, homogenized, and lysed. Protein concentrations were controlled using Bradford assays. Equal amounts of protein lysates were used to measure both the luciferase (as an internal control) and β-galactosidase activities in a dual-light chemiluminescent reporter gene assay system (Tropix Inc.). In some experiments, equal amounts of protein lysates were loaded onto SDS-PAGE gels and blotted with the rabbit polyclonal anti-GFP antibody AB3080 (Chemicon Inc.; for visualizing various GFP–Smo fusions) and the mouse monoclonal anti-β tubulin antibody TU27 (Babco; for the loading control).

For direct observation of GFP-tagged proteins, salivary glands were dissected from early wandering thirdinstar larvae, fixed and quenched as described previously. 7-aminoactinomycin-D (7AAD; Molecular Probes) was used to mark nuclei. Specimens were examined in a Bio-Rad confocal microscope. For the measurement of relative fluorescence intensity, surface and intracellular compartments of a salivary gland cell were traced using MetaMorph software (Universal Imaging), which measured the area of each compartment and assigned a linear value of average fluorescence intensity. The total fluorescence intensity of each compartment was calculated, scoring 10–15 cells from each transgenic gland.

For salivary gland cultures, UAS–*gfp–smo*/71B salivary glands were dissected and cultured at 25°C in clone 8 (cl-8) cell medium (van Leeuwen et al. 1994). Recombinant HhN protein (5 μg/mL; Biogen)-activated Octyl-HhN (OS-7, a gift from Ontogeny, Inc.), or concentrated conditioned medium from S2 cells producing HhN was added for 20–30 min. In some experiments, 40 μM nocodazole (Sigma) or 1 μM latrunculin A (Molecular Probes) was added to the gland cultures for 2 h before the addition of HhN, to destroy microtubules or the actin cytoskeleton. Controls to show successful perturbation of the cytoskeleton employed drug-treated glands incubated with either monoclonal anti-tubulin antibody TU27 or anti-actin antibody C4 (Chemicon). To inhibit protein synthesis, 100 μM cycloheximide (Sigma) was added for 1–2 h before adding HhN. In some experiments, salivary glands were treated with the phosphatase inhibitors okadaic acid (100 nM; Sigma) or calyculin A (20 *v*M; Sigma) for 2 h. In some experiments, salivary gland cells expressing KKDE-fusions were immunolabeled with the mouse monoclonal anti-protein disulfide isomerase antibody SPA-891 (StressGen Biotech., San Diego, CA) to confirm the correct ER localization.

Cell cultures and transfection

cl-8 cells were cultured as described in van Leeuwen et al. (1994). The *gfp–smo* cDNA was cloned into the pMK33 expression vector (Lee et al. 1994). Transient transfection was performed using CellFectin transfection reagent (Life Technologies, Gaithersburg, MD). The HhN-producing S2 cell line was a gift from P. Beachy (Lee et al. 1994). Conditioned medium was collected from HhN–S2 or control S2 cells induced with 0.5 mM $CuSO_4$ in cl-8 medium without hygromycin B for 24 h. Transfected cl-8 cells were treated with HhN or control conditioned medium for 24 h. Cells were fixed in 4% formaldehyde for 20 min at room temperature and examined with confocal microscopy.

Acknowledgments

We thank Matt Fish for help in making transgenic flies; Charlene Kon, Liqun Luo, Roel Nusse, Anthony Oro, and Michael Simon for insightful critiques of the manuscript; and Deborah Andrew, Joan Hooper, Dennis Ko, and Suzanne Pfeffer for helpful discussions. We thank Philip Beachy, Amy Bejsovec, Suzanne Eaton, Marcos González-Gaitán, Philip Ingham, Yuh Nung Jan, and Ronald Johnson for generous help with fly stocks, cells, and other supplies. A.J.Z. was supported by a Human Frontier Science Program Long-term Postdoctoral Fellowship

(LT0229/1999-M) and a Walter and Idun Berry Fellowship for children's health. L.Z. was supported by a Jane Coffin Childs Memorial Fund for Medical Research Fellowship. The research reported here was supported by the Howard Hughes Medical Institute. M.P.S. is an Investigator of the H.H.M.I.

The publication costs of this article were defrayed in part by payment of page charges. This article must therefore be hereby marked "advertisement" in accordance with 18 USC section 1734 solely to indicate this fact.

References

Alcedo, J., Zou, Y., and Noll, M. 2000. Posttranscriptional regulation of smoothened is part of a self-correcting mechanism in the Hedgehog signaling system. *Mol. Cell* **6:** 457–465.

Andrew, D.J., Henderson, K.D., and Seshaiah, P. 2000. Salivary gland development in *Drosophila melanogaster*. *Mech. Dev.* **92:** 5–17.

Bailey, E.C., Scott, M.P., and Johnson, R.L. 2000. Hedgehog signaling in animal development and human disease. *Ernst Schering Res. Found. Workshop* **29:** 211–235.

Benting, J.H., Rietveld, A.G., and Simons, K. 1999. N-Glycans mediate the apical sorting of a GPI-anchored, raft-associated protein in Madin-Darby canine kidney cells. *J. Cell Biol.* **146:** 313–320.

Bucci, C., Parton, R.G., Mather, I.H., Stunnenberg, H., Simons, K., Hoflack, B., and Zerial, M. 1992. The small GTPase Rab5 functions as a regulator factor in the early endocytic pathway. *Cell* **70:** 715–728.

Chen, J.K., Taipale, J., Cooper, M.K., and Beachy, P.A. 2002. Inhibition of Hedgehog signaling by direct binding of cyclopamine to Smoothened. *Genes & Dev.* **16:** 2743–2748.

Clark, I.E., Jan, L.Y., and Jan, Y.N. 1997. Reciprocal localization of Nod and kinesin fusion proteins indicates microtubule polarity in the *Drosophila* oocyte, epithelium, neuron and muscle. *Development* **124:** 461–470.

DeCamp, D.L., Thompson, T.M., de Sauvage, F.J., and Lerner, M.R. 2000. Smoothened activates Gα-mediated signaling in frog melanophores. *J. Biol. Chem.* **275:** 26322–26327.

Denef, N., Neubuser, D., Perez, L., and Cohen, S.M. 2000. Hedgehog induces opposite changes in turnover and subcellular localization of Patched and Smoothened. *Cell* **102:** 521–531.

Eggenschwiler, J.T., Espinoza, E., and Anderson, K.V. 2001. Rab23 is an essential negative regulator of the mouse Sonic hedgehog signalling pathway. *Nature* **412:** 194–198.

Entchev, E.V., Schwabedissen, A., and González-Gaitán, M. 2000. Gradient formation of the TGF-β homolog DPP. *Cell* **103:** 981–991.

Forbes, A.J., Nakano, Y., Taylor, A.M., and Ingham, P.W. 1993. Genetic analysis of Hedgehog signalling in the *Drosophila* embryo. *Dev. Suppl.* 115–124.

Greco, V., Hannus, M., and Eaton, S. 2001. Argosomes: A potential vehicle for the spread of morphogens through epithelia. *Cell* **106:** 633–645.

Hammerschmidt, M. and McMahon, A.P. 1998. The effect of pertussis toxin on zebrafish development: A possible role for inhibitory G-proteins in Hedgehog signaling. *Dev. Biol.* **194:** 166–171.

Incardona, J.P., Gruenberg, J., and Roelink, H. 2002. Sonic hedgehog induces the segregation of Patched and Smoothened in endosomes. *Curr. Biol.* **12:** 983–995.

Ingham, P.W. and Fietz, M.J. 1995. Quantitative effects of *hedgehog* and *decapentaplegic* activity on the patterning of the *Drosophila* wing. *Curr. Biol.* **5:** 432–440.

Ingham, P.W. and McMahon, A.P. 2001. Hedgehog signaling in animal development: paradigms and principles. *Genes Dev.* **15:** 3059–3087.

Ingham, P.W., Nystedt, S., Nakano, Y., Brown, W., Stark, D., van den Heuvel, M., and Taylor, A.M. 2000. Patched represses the Hedgehog signalling pathway by promoting modification of the Smoothened protein. *Curr. Biol.* **10:** 1315–1318.

Ioannou, Y.A. 2001. Multidrug permeases and subcellular cholesterol transport. *Nat. Rev. Mol. Cell Biol.* **2:** 657–668.

Johnson, R.L., Grenier, J.K., and Scott, M.P. 1995. *patched* overexpression alters wing disc size and pattern: Transcriptional and post-transcriptional effects on *hedgehog* targets. *Development* **121:** 4161–4170.

Johnson, R.L., Milenkovic, L., and Scott, M.P. 2000. In vivo functions of the Patched protein: Requirement of the C terminus for target gene inactivation but not Hedgehog sequestration. *Mol. Cell* **6:** 467–478.

Kalderon, D. 2000. Transducing the hedgehog signal. *Cell* **103:** 371–374.

Lee, J.J., Ekker, S.C., von Kessler, D.P., Porter, J.A., Sun, B.I., and Beachy, P.A. 1994. Autoproteolysis in hedgehog protein biogenesis. *Science* **266:** 1528–1537.

Lotti, L.V., Mottola, G., Torrisi, M.R., and Bonatti, S. 1999. A different intracellular distribution of a single reporter protein is determined at steady state by KKXX or KDEL retrieval signals. *J. Biol. Chem.* **274:** 10413–10420.

Lu, Z.L., Saldanha, J.W., and Hulme, E.C. 2002. Seven-transmembrane receptors: Crystals clarify. *Trends Pharmacol. Sci.* **23:** 140–146.

McKay, R.R., Zhu, L., and Shortridge, R.D. 1995. A *Drosophila* gene that encodes a member of the protein disulfide isomerase/phospholipase-Cα family. *Insect Biochem. Mol. Biol.* **25:** 647–654.

McLauchlan, H., Newell, J., Morrice, N., Osborne, A., West, M., and Smythe, E. 1998. A novel role for Rab5-GDI in ligand sequestration into clathrin-coated pits. *Curr. Biol.* **8:** 34–45.

Martín, V., Carrillo, G., Torroja, C., and Guerrero, I. 2001. The sterol-sensing domain of Patched protein seems to control Smoothened activity through Patched vesicular trafficking. *Curr. Biol.* **11:** 601–607.

Moline, M.M., Southern, C., and Bejsovec, A. 1999. Directionality of Wingless protein transport influences epidermal patterning in the *Drosophila* embryo. *Development* **126:** 4375–4384.

Muñiz, M. and Riezman, H. 2000. Intracellular transport of GPI-anchored proteins. *EMBO J.* **19:** 10–15

Munro, S. and Pelham, H.R. 1987. A C-terminal signal prevents secretion of luminal ER proteins. *Cell* **48:** 899–907.

Nybakken, K. and Perrimon, N. 2002. Hedgehog signal transduction: Recent findings. *Curr. Opin. Genet. Dev.* **12:** 503.

Porter, J.A., von Kessler, D.P., Ekker, S.C., Young, K.E., Lee, J.J., Moses, K., and Beachy, P.A. 1995. The product of *hedgehog* autoproteolytic cleavage active in local and long-range signalling. *Nature* **374:** 363–366.

Quirk, J., van den Heuvel, M., Henrique, D., Marigo, V., Jones, T.A., Tabin, C., and Ingham, P.W. 1997. The *smoothened* gene and hedgehog signal transduction in *Drosophila* and vertebrate development. *Cold Spring Harb. Symp. Quant. Biol.* **62:** 217–226.

Resh, M.D. 1999. Fatty acylation of proteins: New insights into membrane targeting of myristoylated and palmitoylated proteins. *Biochim. Biophys. Acta* **1451:** 1–16.

Robbins, D.J., Nybakken, K.E., Kobayashi, R., Sisson, J.C., Bishop, J.M., and Therond, P.P. 1997. Hedgehog elicits signal transduction by means of a large complex containing the kinesin-related protein Costal2. *Cell* **90:** 225–234.

Sisson, J.C., Ho, K.S., Suyama, K., and Scott, M.P. 1997. Costal2, a novel kinesin-related protein in the Hedgehog signaling pathway. *Cell* **90:** 235–245.

Somsel Rodman, J. and Wandinger-Ness, A. 2000. Rab GTPases coordinate endocytosis. *J. Cell Sci.* **113:** 183–192.

Stegman, M.A., Vallance, J.E., Elangovan, G., Sosinski, J., Cheng, C., and Robbins, D.J. 2000. Identification of a tetrameric Hedgehog signaling complex. *J. Biol. Chem.* **275:** 21809–21812.

Strittmatter, S.M., Igarashi, M., and Fishman, M.C. 1994. GAP-43 amino terminal peptides modulate growth cone morphology and neurite outgrowth. *J. Neurosci.* **14:** 5503–5513.

Strutt, H., Thomas, C., Nakano, Y., Stark, D., Neave, B., Taylor, A.M., and Ingham, P.W. 2001. Mutations in the sterol-sensing domain of Patched suggest a role for vesicular trafficking in Smoothened regulation. *Curr. Biol.* **11:** 608–613.

Taipale, J., Chen, J.K., Cooper, M.K., Wang, B., Mann, R.K., Milenkovic, L., Scott, M.P., and Beachy, P.A. 2000. Effects of oncogenic mutations in *Smoothened* and *Patched* can be reversed by cyclopamine. *Nature* **406:** 1005–1009.

Taipale, J., Cooper, M.K., Maiti, T., and Beachy, P.A. 2002. Patched acts catalytically to suppress the activity of Smoothened. *Nature* **418:** 892–897.

van der Bliek, A.M., Redelmeier, T.E., Damke, H., Tisdale, E.J., Meyerowitz, E.M., and Schmid, S.L. 1993. Mutations in human dynamin block an intermediate stage in coated vesicle formation. *J. Cell Biol.* **122:** 553–563.

van Leeuwen, F., Samos, C.H., and Nusse, R. 1994. Biological activity of soluble Wingless protein in cultured *Drosophila* imaginal disc cells. *Nature* **368:** 342–344.

Vitelli, R., Santillo, M., Lattero, D., Chiariello, M., Bifulco, M., Bruni, C.B., and Bucci, C. 1997. Role of the small GTPase Rab7 in the late endocytic pathway. *J. Biol. Chem.* **272:** 4391–4397.

Xie, J., Murone, M., Luoh, S.M., Ryan, A., Gu, Q., Zhang, C., Bonifas, J.M., Lam, C.W., Hynes, M., Goddard, A., et al. 1998. Activating *Smoothened* mutations in sporadic basal-cell carcinoma. *Nature* **391:** 90–92.